

Application Article

Low Profile EBG Resonator Antennas

R. Chantalat,¹ L. Moustafa,² M. Thevenot,² T. Monediere,² and B. Jecko²

¹ Centre d'Ingénierie des Systèmes en Télécommunication, en ÉlectroMagnétisme et en Électronique (CISTEME), Faculté des Sciences, Université de Limoges, 123 rue Albert Thomas, 87060 Limoges Cedex, France

² Ondes et Systèmes Associés (OSA), Department of XLIM Laboratory, Faculté des Sciences, Université de Limoges, 123 rue Albert Thomas, 87060 Limoges Cedex, France

Correspondence should be addressed to R. Chantalat, regis.chantalat@cisteme.net

Received 21 June 2008; Revised 5 December 2008; Accepted 30 March 2009

Recommended by Hisashi Morishita

An Electromagnetic Band Gap (EBG) antenna is a planar structure which is composed of a cavity and an EBG material. In most applications, the height of the EBG antenna is half wavelength. We present in this paper the conditions to reduce the profile of an EBG antenna to subwavelength values. It could be achieved by using a cavity upper interface which exhibits negative reflection phase. Frequency Selective Surface (FSS) based on Babinet principle, that satisfies this condition, will be described using full wave analysis. These periodic metallic arrays are employed in the design of a low profile EBG antenna which has a directivity of 10 dBi. As this EBG antenna design is similar to a small antenna over an Artificial Magnetic Conductors (AMC) surfaces or High Impedance Surface (HIS), the EBG antenna principle could be a new theory approach for the AMC or HIS. This point is discussed in this paper.

Copyright © 2009 R. Chantalat et al. This is an open access article distributed under the Creative Commons Attribution License, which permits unrestricted use, distribution, and reproduction in any medium, provided the original work is properly cited.

1. Introduction

Recent papers [1–7] show the radiation of small antennas located very near ($\cong \lambda/15$) high impedance surfaces or EBG reflectors. In many cases, these textured surfaces which are presented as AMC surfaces are built with at least one FSS connected or not to a ground plane. These AMC surfaces act as Perfect Magnetic Conductors (PMC) over a narrow frequency band. The PMC surface which is, electromagnetically the dual surface of an PEC surface, exhibits a reflection coefficient of $\rho = +1$. Consequently, the currents image for PMC is in phase with the original currents. This allows to utilize PMCs as reflectors, and to place radiating elements very close to the PMC thus resulting in low profile antennas. AMC surfaces consist in general of a lattice of metallic plates printed on a grounded dielectric substrate. AMC surfaces which incorporate vias connecting the patches to the ground plane, have been designed to suppress the propagation of surface waves because of the Transverse Electric (TE) mode band gap [6, 7]. In this paper, we propose a new theory approach of this kind of structures based on EBG resonator antenna principle. We will demonstrate that a structure composed of periodic metallic plates placed very close to

a ground plane could be considered as a low profile EBG resonator antenna. In this condition, the array acts as a partially reflective surface that forms a resonant cavity with the ground plane. The low profile EBG resonator antenna is an EBG resonator antenna [8–10] which has a very small height in comparison to the wavelength: approximatively $\lambda/15$ instead of $\lambda/2$ for a usual EBG antenna. First, the EBG resonator antenna working is briefly reminded. Then, the design of the EBG material which permits to reduce the profile of the EBG antenna is described. Finally, low profile EBG antenna performances are given.

2. EBG Resonator Antenna

An EBG resonator antenna is a high gain planar antenna that behaves like a radiating aperture [8–11]. This antenna is composed of an EBG material and a ground plane which form a longitudinal resonator (Figure 1). Electromagnetic probe that could be a patch or a dipole is introduced into the resonator to excite the structure. The operating frequency f_0 is defined by the longitudinal resonance in the z direction

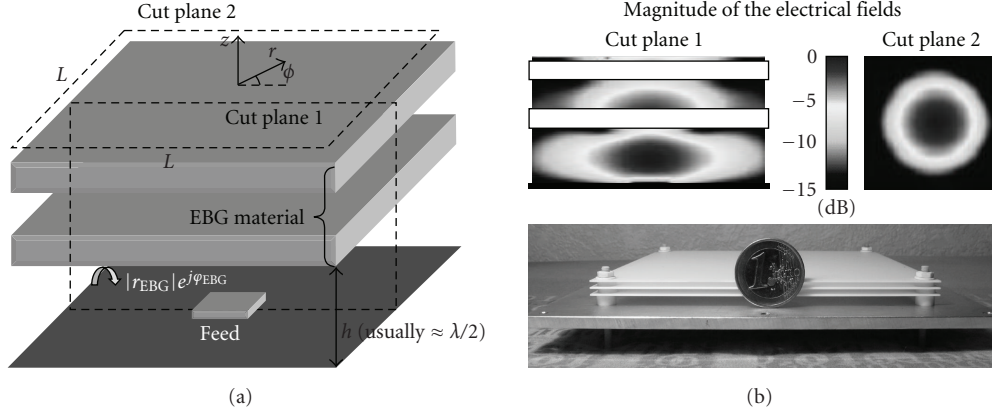


FIGURE 1: (a) Schematic view of an EBG resonator antenna; (b) EM fields at the operating frequency.

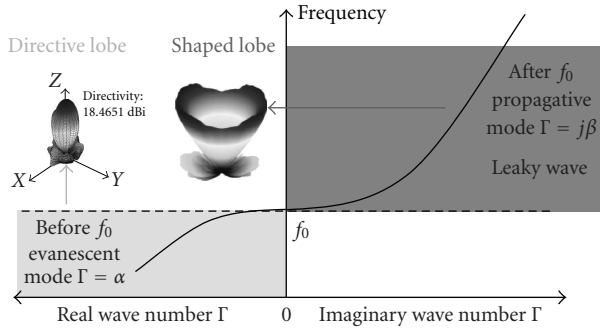


FIGURE 2: Dispersion diagram of the EBG antenna.

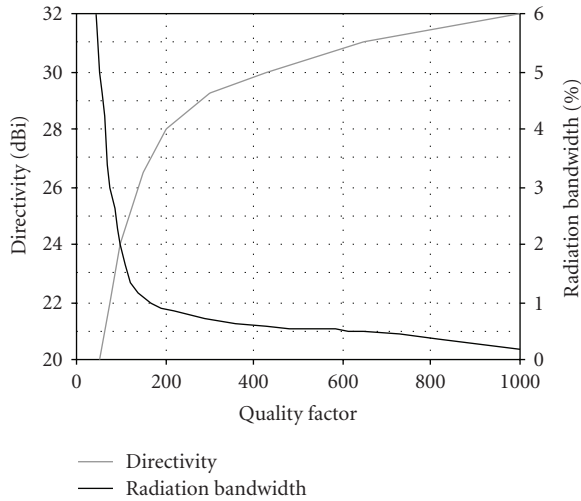


FIGURE 3: Directivity and radiation bandwidth.

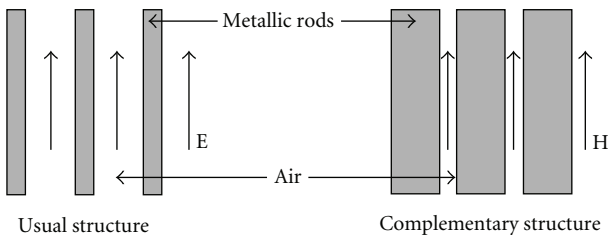


FIGURE 4: Babinet theorem.

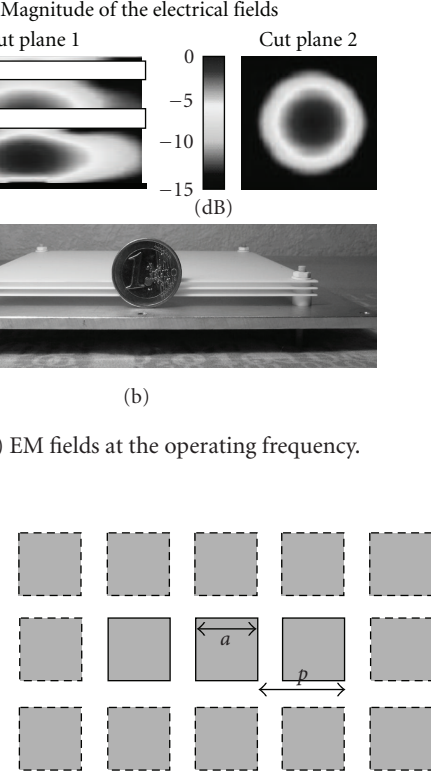


FIGURE 5: FSS composed of an array of square patches.

and it depends of the reflection phase of the upper interface φ_{EBG} and the height h as shown by (1),

$$f_0 = \frac{c}{2h} \left(\frac{\varphi_{\text{EBG}}(f_0) + \pi}{2\pi} \right), \quad (1)$$

$$Q = \frac{\sqrt{|r_{\text{EBG}}(f_0)|}}{1 - |r_{\text{EBG}}(f_0)|} \left(\frac{\varphi_{\text{EBG}}(f_0) + \pi}{2} \right). \quad (2)$$

As f_0 indicates the cut off frequency of the fundamental plane waveguide mode, the available frequency range is located towards f_0 in order to have directive main lobe (Figure 2) [10, 11]. Indeed, the structure behaves like a leaky wave antenna above f_0 because the mode is propagating in the transverse radial direction r . In this case, shaped radiation patterns are obtained because the propagation constant induces some angle pointing from the broadside direction (Figure 2) [12]. Also, the EBG antenna behaves like a radiating aperture only towards f_0 , because the mode is evanescent in the radial direction r [10, 11]. Indeed, electromagnetic fields decay with an exponential law around the feed leading to a Gaussian distribution upper the antenna (Figure 1(b)).

The attenuation coefficient α of the evanescent mode that influences the size of the equivalent aperture (and then the gain) depends on the quality factor Q of the resonator. As explained in (2), this last one is strongly impacted by the reflection coefficient of the EBG material at the operating frequency f_0 ($|r_{\text{EBG}}| e^{j\varphi_{\text{EBG}}}$). Several FDTD simulations have permitted to deduce the EBG antenna potential directivity and the half radiation bandwidth as a function of the

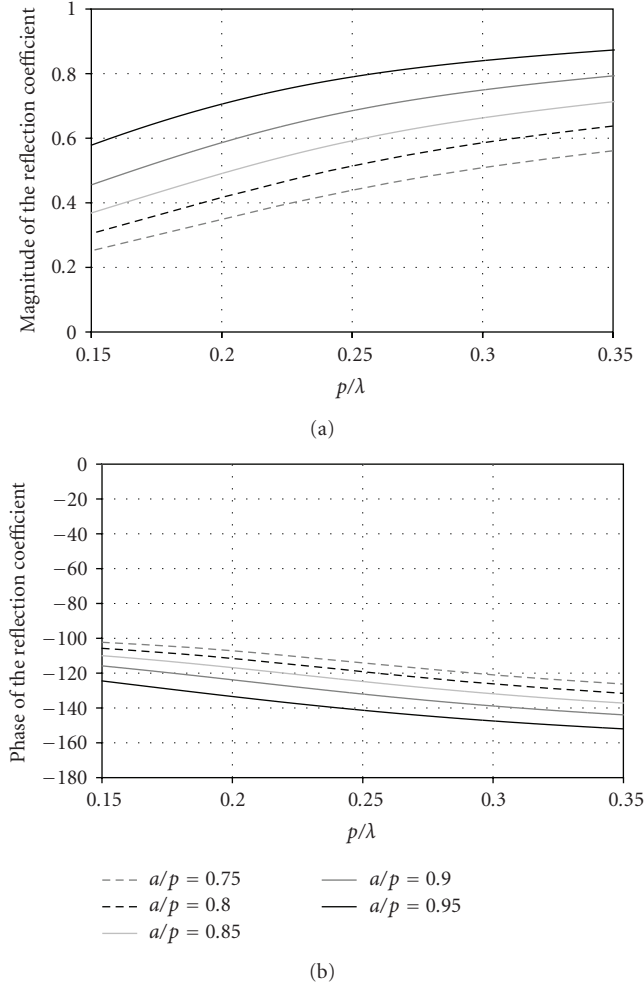


FIGURE 6: Reflection coefficient of the FSS.

resonator quality factor (Figure 3) [9–11]. The line graph of radiation bandwidth is available for conventional EBG material (dielectric layers or nonresonant FSS) that has a smooth variation of the reflection phase as function of the frequency. As the EBG antenna behaves like a radiating aperture, its lateral dimension L must verify the formula (3) to obtain the expected directivity D given in Figure 3. This condition allows an ideal Gaussian distribution of the electromagnetic field above the EBG antenna with a low level on the edges [9]. The profile of an EBG antenna is always close to a half wavelength because the conventional EBG material has a reflection coefficient which tends to $1e^{j\varphi\pi}$ [8–11]. In this paper, the goal is to reduce the height of the EBG antenna to subwavelength values. According to (4), this required condition is to use an EBG material that has a negative reflection phase. The next paragraph is dedicated to the study of an FSS that agrees with this requirement:

$$L \geq \sqrt{\frac{1}{80f_0^2} \times 10^{D_{\text{dB}}/10}}, \quad (3)$$

$$h = \frac{c}{2f_0} \left(\frac{\varphi_{\text{up}}(f_0) + \pi}{2\pi} \right). \quad (4)$$

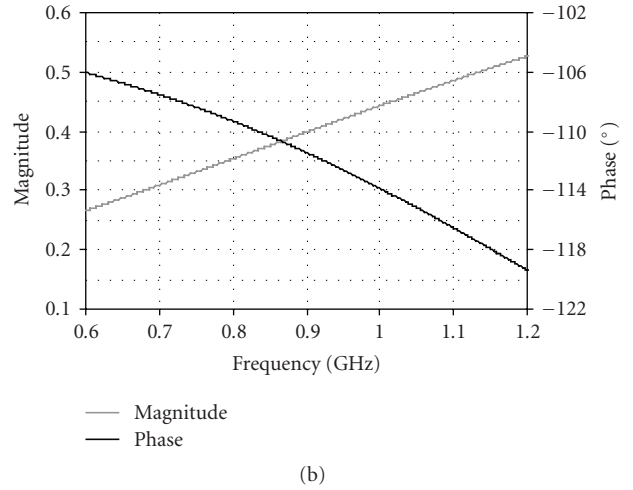
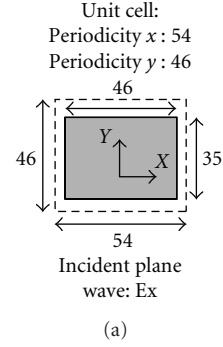


FIGURE 7: Reflection coefficient of the FSS.

3. Low Profile EBG Resonator Antenna

3.1. Design of the FSS. The profile of the EBG antenna could be reduced if the reflection phase φ_{EBG} is negative according to (4). Usually, a metallic EBG material is a frequency selective surface (FSS) composed of metallic rods that are thin and parallel to the E field of the feed [10, 11]. This structure is a high pass filter and has a reflection phase near to π for the low frequencies. The Babinet theorem has been applied on the conventional FSS in order to obtain a low pass filter (Figure 4). Also, we have studied the complementary form of a metallic grid that is an array of squares patches closely arranged (Figure 5).

The reflection coefficient has been studied using periodic boundary conditions in CST Microwave studio in order to limit the computational space to a single unit cell (Figure 6). The periodicity p is normalized to the wavelength and the length of the patches a is normalized to the periodicity p . We can see in Figure 6 that the “Babinet surface” is a low pass filter which presents a negative reflection phase. The higher the periodicity or the patch length, the more important the reflection coefficient magnitude and the more the phase tends to $-\pi$. However, whatever the used FSS, the directivity of the EBG antenna will be low and the radiation bandwidth will be high because of the weak quality factor (2). In order to design a low profile EBG antenna operating at 0.9 GHz, a Babinet surface which dimensions are given in Figure 7

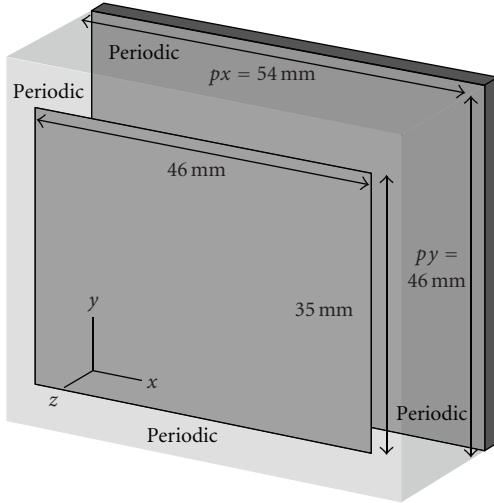


FIGURE 8: Periodic structure.

has been chosen. As its coefficient reflection phase is near to -112° at 0.9 GHz, the theoretical value of the resonator height should be 30 mm ($\approx \lambda/10$).

3.2. Dispersion Diagram. The unit cell of the FSS (Figure 7) has been placed at 30 mm above a PEC surface (Figure 8). This periodic structure has been characterized with an “in house” software in order to obtain the dispersion diagram of the modes supported by this low profile resonator. We can see in Figure 9 that two modes propagate in the frequency range [0–1.4 GHz]. The first is a surface wave that has no cut off frequency. As predicted in Section 3.1, an EBG mode propagates in the low profile resonator above the cut off frequency that is equals to 0.94 GHz. Obviously, the EBG mode is evanescent below this frequency. Consequently, subwavelength EBG cavity can be achieved by incorporating Babinet FSS with negative reflection phase response.

3.3. Low Profile EBG Antenna. The unit cell given in Figure 7 is applied in the design of an EBG antenna operating at 0.9 GHz. The low profile EBG antenna design is composed of a 20 mm air resonator ($\approx \lambda/15$) and an FSS with 100 cells (Figure 10). This value is a little different from the predicted value given in Section 3.1 because the structure is not infinite. The overall size of 540 mm by 450 mm is sufficient; respecting the condition given in (3) because the field level located at the edge of the antenna is weak (Figure 11). We can see in this figure that the field distribution inside the EBG resonator at the operating frequency reveals the usual exponential decay in the transverse direction.

As explained in [9], the EBG antenna matching depends on the feed and the resonator quality factor. So, it is necessary to optimize the dimensions of the feed in order to adjust its resonance frequency. This last is a key parameter in the matching procedure and a set of simulations permits to obtain the best configuration. In our case, the feed is a dipole located at 6 mm above the Babinet surface and its length is equal to 125 mm. These dimensions that induce a half

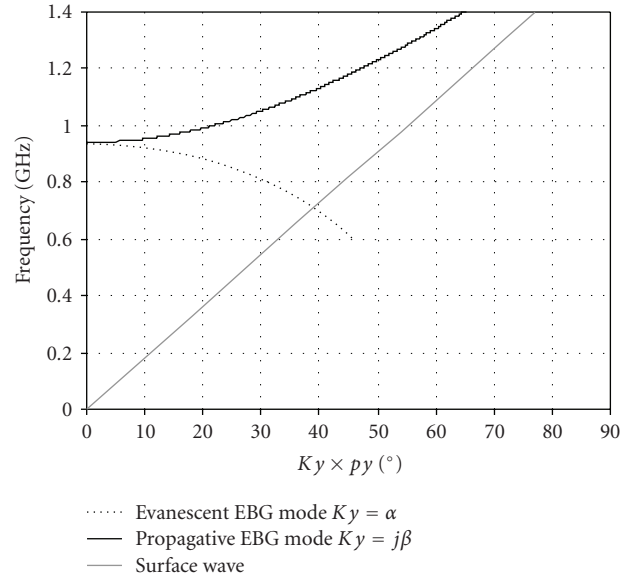


FIGURE 9: Dispersion diagram of the low profile EBG resonator.

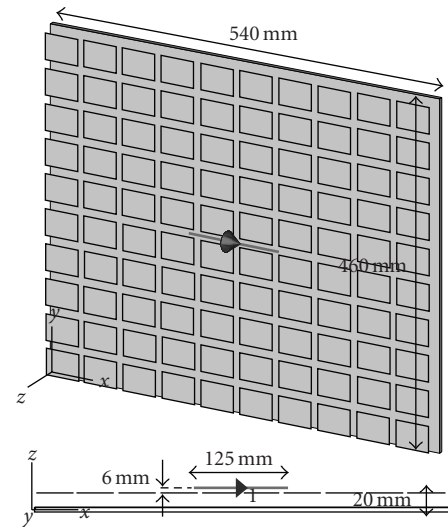


FIGURE 10: Low profile EBG resonator antenna.

wavelength resonance at 0.97 GHz (Figure 12) have been chosen in order to match the EBG antenna in the frequency range where the directivity is the most important (Figure 14). We can notice that this resonance frequency is different from the one in free space because of the EBG material and the ground plane influences. The 7% matching bandwidth is a usual result for an EBG antenna (Figure 13). But this value is very low compared to the -3 dB directivity bandwidth near to 100% (Figure 14). However, it is possible to match the EBG over a wider bandwidth under some conditions which are explained in Section 3.4.

In Figure 15, the radiation pattern of the EBG antenna at 0.9 GHz exhibits an axial main lobe with a directivity of 10 dBi. The wide bandwidth and the weak directivity result from the weak quality factor. The radiation patterns

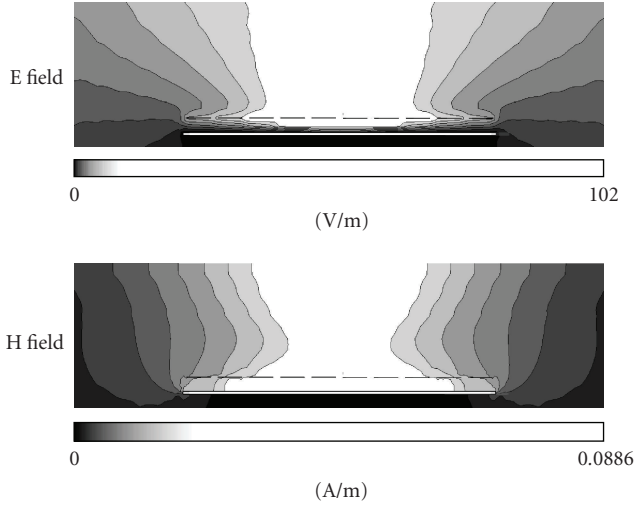


FIGURE 11: Field distribution in the E and H-plane at 0.9 GHz.

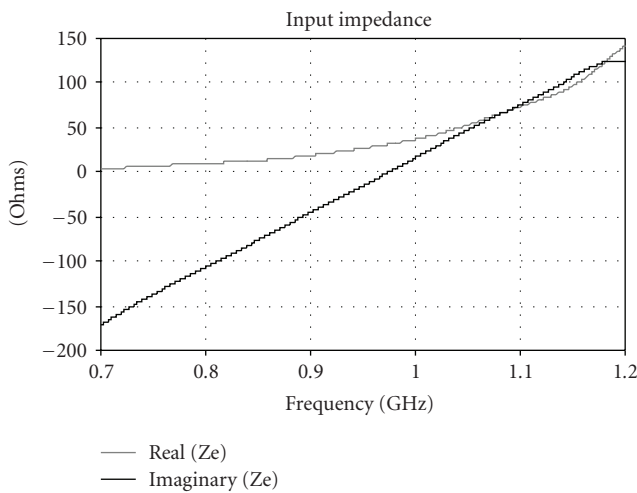


FIGURE 12: Input impedance.

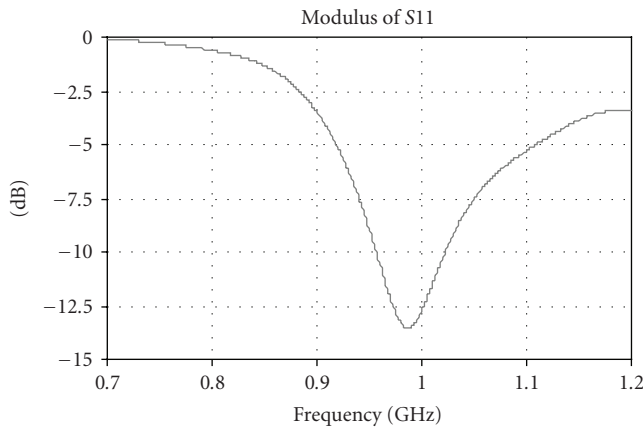


FIGURE 13: Antenna matching ($|S_{11}|$).

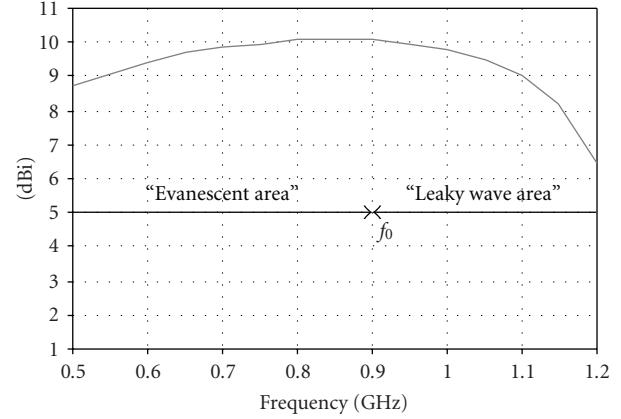


FIGURE 14: Directivity versus frequency.

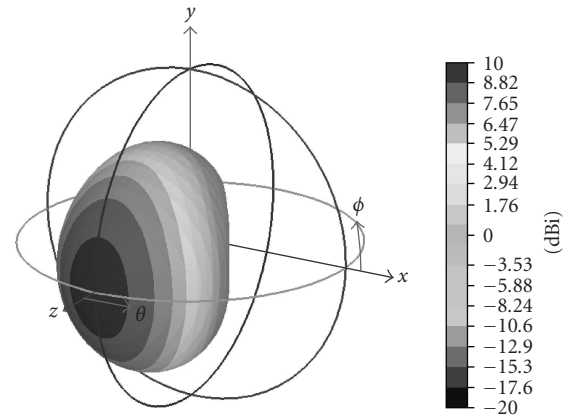


FIGURE 15: Radiation pattern at 0.9 GHz.

at different frequencies in the E (Figure 16) and H-plane (Figure 17) are the same as for a classical $\lambda/2$ EBG antenna.

As explained in Section 2, in the “evanescent area” located below the resonance frequency given by (1), an axial main lobe is obtained because of the exponential decay of the fields in the transverse direction (Figure 11). Obviously, the maximum directivity is obtained for the frequency at 0.9 GHz. Below this value, the directivity is a decreasing function of the frequency because the attenuation coefficient α of the evanescent mode increases (Figure 9). For the frequencies over the cut off frequency in the “leaky wave area”, a main lobe with two peaks is obtained in the propagation plane. As explained in [12], the angular deviation from the boresight direction depends on the propagation constant of the mode. As this last is equal to $17, 45 \text{ m}^{-1}$ at 1.2 GHz (Figure 9), the theoretical value is 42° . The difference with the angular deviation that has been obtained in the simulated radiation pattern at 1.2 GHz is to 5° .

3.4. Feeding Source. In the design described above, the feeding dipole is located at 6 mm over the FSS. However, the small antenna (dipole, patch, etc.) which is used to feed the low profile EBG resonator antenna can be located inside or outside the resonator without modifying its behavior. In

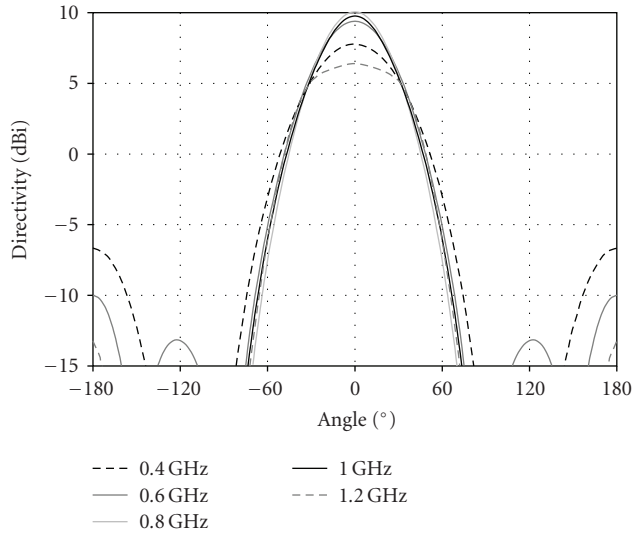


FIGURE 16: Radiation patterns in the E-plane.

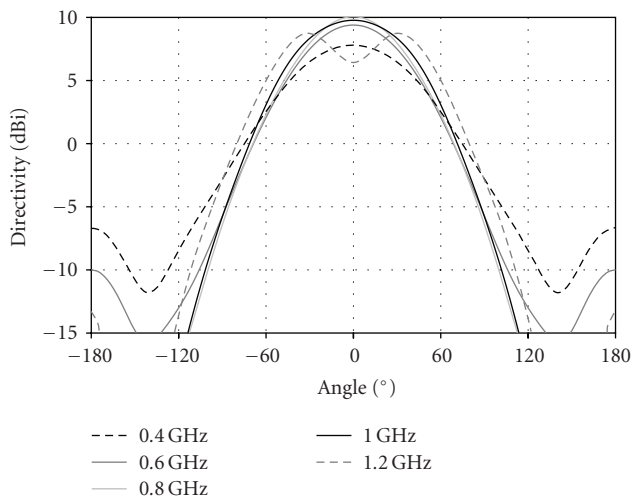


FIGURE 17: Radiation patterns in the H-plane.

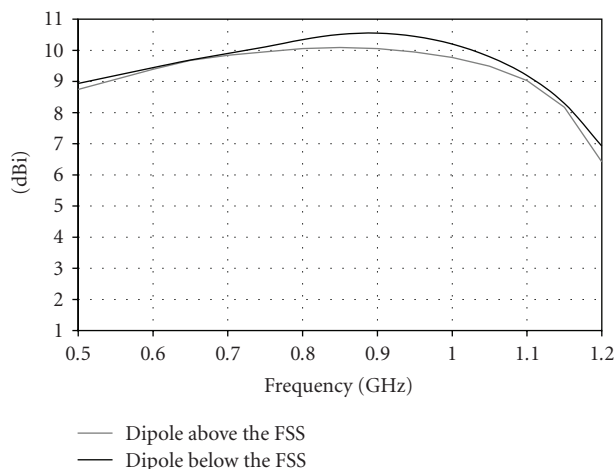


FIGURE 18: Antenna directivity versus the dipole location.

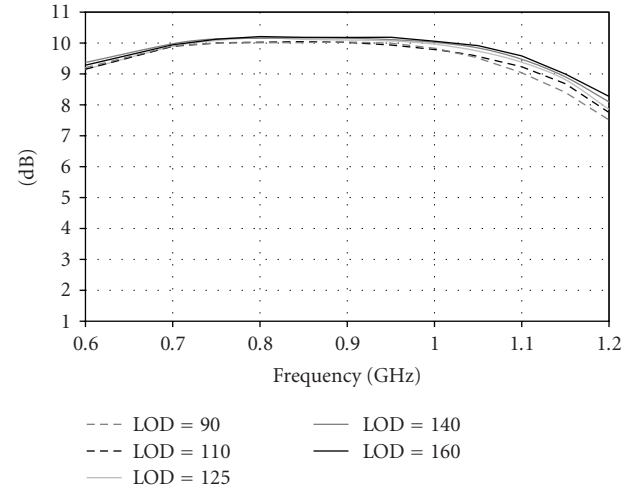


FIGURE 19: Directivity versus the dipole length.

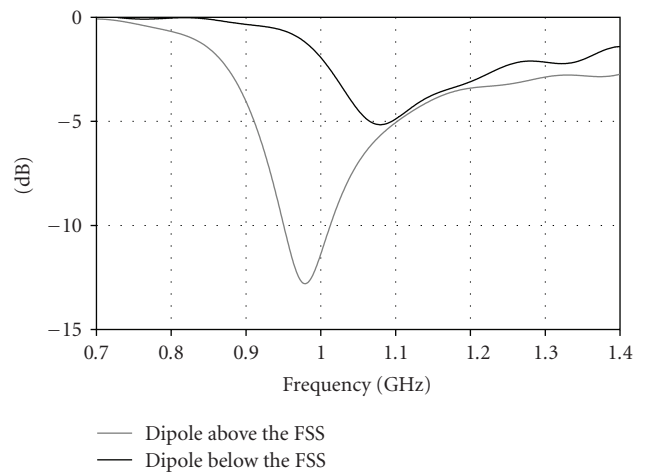


FIGURE 20: Antenna matching versus the dipole location.

Figure 18, the directivity of the low profile EBG antenna excited by a dipole located under the FSS is the same as for previous result obtained with the dipole over the FSS. Moreover, the dipole length LOD has no influence on the radiation performances of the EBG antenna (Figure 19). That means that the structure radiation is not the radiation of the dipole modified by the presence of a high impedance surface as explained in [1–7]. But, it is the radiation of the low profile EBG antenna itself.

However, the feeding dipole impacts strongly the EBG antenna matching. Indeed, we can see that the input coefficient reflection depends on the dipole location. In these two cases, the dipole length is 125 mm and its distance to the FSS is 6 mm. But in the case of the dipole under the FSS, its location very close to the ground plane induces a weak input impedance magnitude resulting in bad matching (Figure 20). Also, as explained in [9], it is necessary to compute all the feed parameters to find the appropriate configuration. However, the matching procedure is always easier in the leaky wave area (located after f_0

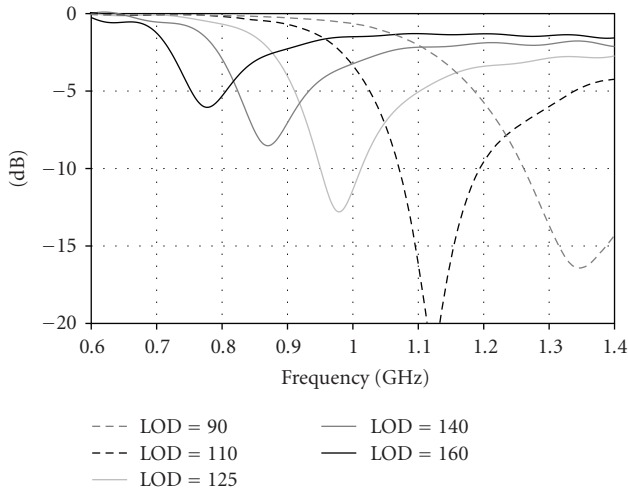


FIGURE 21: Antenna matching versus the dipole length.

that corresponds to the maximum directivity) because of the mode propagation. As shown in Figure 21 that reveals the input reflection coefficient as function of the dipole length, the more evanescent the mode is, the harder the matching procedure is. Consequently, it is possible to match the antenna over a large bandwidth as seen in some HIS papers [2, 5] but in this case the directivity of the antenna is not important.

4. Conclusion

Frequency Selective Surface based on the Babinet principle has been applied to design a low profile EBG resonator antenna. It was derived theoretically that subwavelength EBG cavity antennas can be achieved by incorporating periodic rectangular sheets with negative reflection phase response. The use of a Babinet surface with reflection phase -110° results in a thin $\lambda/15$ EBG antenna with a directivity of 10 dBi. This low directivity and the large radiation bandwidth ($\approx 100\%$) are explained by the low quality factor of the resonator. We have shown too the difficult matching procedure of this kind of antenna in the “evanescent area” where the main lobe is directive. The designed low profile EBG antenna has the same composition as well known structures with small antennas located over an artificial magnetic conductor surface. So, the behavior of these last structures could be explained by a new theory approach based on EBG antenna principle.

References

- [1] F. Yang and Y. Rahmat-Samii, “Reflection phase characterizations of the EBG ground plane for low profile wire antenna applications,” *IEEE Transactions on Antennas and Propagation*, vol. 51, no. 10, pp. 2691–2703, 2003.
- [2] H. Nakano, K. Hitosugi, N. Tatsuzawa, D. Togashi, H. Mimaki, and J. Yamauchi, “Effects on the radiation characteristics of using a corrugated reflector with a helical antenna and an electromagnetic band-gap reflector with a spiral antenna,” *IEEE Transactions on Antennas and Propagation*, vol. 53, no. 1, pp. 191–199, 2005.
- [3] Y. Zhang, J. von Hagen, M. Younis, C. Fischer, and W. Wiesbeck, “Planar artificial magnetic conductors and patch antennas,” *IEEE Transactions on Antennas and Propagation*, vol. 51, no. 10, pp. 2704–2712, 2003.
- [4] M. Hosseini, A. Pirahadi, and M. Hakkak, “Design of a non uniform high impedance surface for a low profile antenna,” in *Progress in Electromagnetics Research Symposium*, pp. 352–356, Cambridge, Mass, USA, March 2006.
- [5] D. Sievenpiper, L. Zhang, R. F. J. Broas, N. G. Alexopoulos, and E. Yablonovitch, “High-impedance electromagnetic surfaces with a forbidden frequency band,” *IEEE Transactions on Microwave Theory and Techniques*, vol. 47, no. 11, pp. 2059–2074, 1999.
- [6] F. Yang and Y. Rahmat-Samii, “Microstrip antennas integrated with electromagnetic band-gap (EBG) structures: a low mutual coupling design for array applications,” *IEEE Transactions on Antennas and Propagation*, vol. 51, no. 10, pp. 2936–2946, 2003.
- [7] G. Poislane, “Antennas on high impedance ground planes: on the importance of the antenna isolation,” *Progress in Electromagnetics Research*, vol. 41, pp. 237–255, 2003.
- [8] C. Cheype, C. Serier, M. Thevenot, T. Monédière, A. Reineix, and B. Jecko, “An electromagnetic bandgap resonator antenna,” *IEEE Transactions on Antennas and Propagation*, vol. 50, no. 9, pp. 1285–1290, 2002.
- [9] L. Leger, C. Serier, R. Chantalat, M. Thevenot, T. Monédière, and B. Jecko, “1D dielectric electromagnetic band gap (EBG) resonator antenna design,” *Annales des Télécommunications*, vol. 59, no. 3-4, pp. 242–260, 2004.
- [10] C. Menudier, M. Thevenot, T. Monédière, and B. Jecko, “EBG resonator antennas: state of the art and prospects,” in *Proceedings of the 6th International Conference on Antenna Theory and Techniques (ICATT '07)*, pp. 37–43, Sevastopol, Ukraine, September 2007.
- [11] R. Chantalat, C. Menudier, T. Monédière, M. Thevenot, P. Dumon, and B. Jecko, “Enhanced EBG resonator antenna as feed of a reflector antenna in the Ka band,” *Antennas and Wireless Propagation Letters*, vol. 7, pp. 349–353, 2007.
- [12] D. R. Jackson and A. A. Oliner, “Leaky-wave propagation and radiation for a narrow-beam multiple-layer dielectric structure,” *IEEE Transactions on Antennas and Propagation*, vol. 41, no. 3, pp. 344–348, 1993.

